

# A reciprocal tensin-3–cten switch mediates EGF-driven mammary cell migration

Menachem Katz<sup>1</sup>, Ido Amit<sup>1</sup>, Ami Citri<sup>1</sup>, Tal Shay<sup>2</sup>, Silvia Carvalho<sup>3</sup>, Sara Lavi<sup>1</sup>, Fernanda Milanezi<sup>3</sup>, Ljuba Lyass<sup>4</sup>, Ninette Amariglio<sup>5</sup>, Jasmine Jacob-Hirsch<sup>5</sup>, Nir Ben-Chetrit<sup>1</sup>, Gabi Tarcic<sup>1</sup>, Moshit Lindzen<sup>1</sup>, Roi Avraham<sup>1</sup>, Yi-Chun Liao<sup>6</sup>, Patricia Trusk<sup>4</sup>, Asya Lyass<sup>7</sup>, Gideon Rechavi<sup>5</sup>, Neil L. Spector<sup>8</sup>, Su Hao Lo<sup>6</sup>, Fernando Schmitt<sup>3,9</sup>, Sarah S. Bacus<sup>4</sup> and Yosef Yarden<sup>1</sup>

**Cell migration driven by the epidermal growth factor receptor (EGFR) propels morphogenesis<sup>1</sup> and involves reorganization of the actin cytoskeleton<sup>2</sup>. Although *de novo* transcription precedes migration<sup>3,4</sup>, transcript identity remains largely unknown. Through their actin-binding domains, tensins link the cytoskeleton to integrin-based adhesion sites<sup>5</sup>. Here we report that EGF downregulates tensin-3 expression, and concomitantly upregulates cten, a tensin family member that lacks the actin-binding domain<sup>6</sup>. Knockdown of cten or tensin-3, respectively, impairs or enhances mammary cell migration. Furthermore, cten displaces tensin-3 from the cytoplasmic tail of integrin  $\beta_1$ , thereby instigating actin fibre disassembly. In invasive breast cancer, cten expression correlates not only with high EGFR and HER2, but also with metastasis to lymph nodes. Moreover, treatment of inflammatory breast cancer patients with an EGFR/HER2 dual-specificity kinase inhibitor significantly downregulated cten expression. In conclusion, a transcriptional tensin-3–cten switch may contribute to the metastasis of mammary cancer.**

Epidermal growth factor receptor (EGFR) is involved in various cellular processes, including proliferation and motility, and constitutive receptor activation contributes to the transition from a localized primary tumour mass into an invasive state leading to secondary metastases<sup>1,7</sup>. Several mechanisms have been identified, through which EGFR may regulate cell migration. These include transient activation of proteases, kinases, phospholipases and small GTPases<sup>8</sup>. In addition to early signals that follow EGFR activation, cell migration is also regulated by changes in gene expression programmes; the transcription factor complex AP-1 is required for EGF-induced cell migration<sup>9</sup>, and inhibition of either

transcription or translation impairs endothelial cell migration<sup>3,4</sup>. In invasive prostate cancer cells, EGFR modulates the expression of a plasminogen activator (uPAR) and of prostin-1 (ref. 10), but the identity of other genes underlying EGF-induced cell motility remains largely unknown.

To address the identity of EGF-induced genes that are potentially involved in cell migration, we used a previously established transcriptional profiling data set that is derived from EGF-treated human HeLa cells<sup>11</sup>. Analysis of this data set revealed that prolonged EGF treatment induced the expression of various genes that are involved in the regulation of cell adhesion or organization of the actin cytoskeleton (see Supplementary Information, Fig. S1a). In addition, among other alterations, we observed a reduction in transcripts that encode mediators of cell-to-cell interactions (see Supplementary Information, Fig. S1b).

Notably, we observed reciprocal alterations in the expression of two members of the tensin family. This family comprises four proteins (tensin-1, -2 and -3, and cten (C-terminal tensin-like protein)), which are involved in cell migration, and are localized to focal adhesion sites<sup>5,6</sup>. All four tensin family members contain SH2 and PTB domains in their carboxyl termini. Through the PTB domain, tensins interact with the cytoplasmic tail of  $\beta$  integrins, which are transmembrane cell-adhesion molecules. Although tensin-1, -2 and -3 contain an actin-binding domain in their amino termini, cten is a shorter protein that lacks this domain<sup>6</sup>. Following EGF treatment, TNS3 (tensin-3) mRNA undergoes downregulation, whereas TNS4 (cten) expression exhibits remarkable upregulation (Fig. 1a). Notably, expression of TNS1 (tensin-1) is barely detectable, whereas the moderate expression of tensin-2 is unchanged following EGF treatment. Protein immunoblotting confirmed the induction of cten (see Supplementary Information, Fig. S1c). In addition, cell-to-substrate adhesion — a signal that is known to allow cellular migration<sup>12</sup> — induced cten expression through a mechanism that does not involve

<sup>1</sup>Department of Biological Regulation, The Weizmann Institute of Science, Rehovot 76100, Israel; <sup>2</sup>Department of Physics of Complex Systems, The Weizmann Institute of Science, Rehovot 76100, Israel; <sup>3</sup>IPATIMUP – Institute of Molecular Pathology and Immunology of the University of Porto, Porto 4200-465, Portugal; <sup>4</sup>Targeted Molecular Diagnostics, Westmont, Illinois 60559, USA; <sup>5</sup>Department of Pediatric Hemato-Oncology and Functional Genomics, The Chaim Sheba Medical Center and Sackler School of Medicine, Tel Aviv University, Tel Aviv 69978, Israel; <sup>6</sup>Center for Tissue Regeneration and Repair, Department of Orthopaedic Surgery, University of California-Davis, Sacramento, California 95817, USA; <sup>7</sup>Boston University, Boston, Massachusetts 02215, USA; <sup>8</sup>Department of Exploratory Medical Sciences, GlaxoSmithKline, Research Triangle Park, North Carolina 27709; <sup>9</sup>Medical Faculty of Porto University, Porto 4200-465, Portugal  
Correspondence should be addressed to Y.Y. (yosef.yarden@weizmann.ac.il)

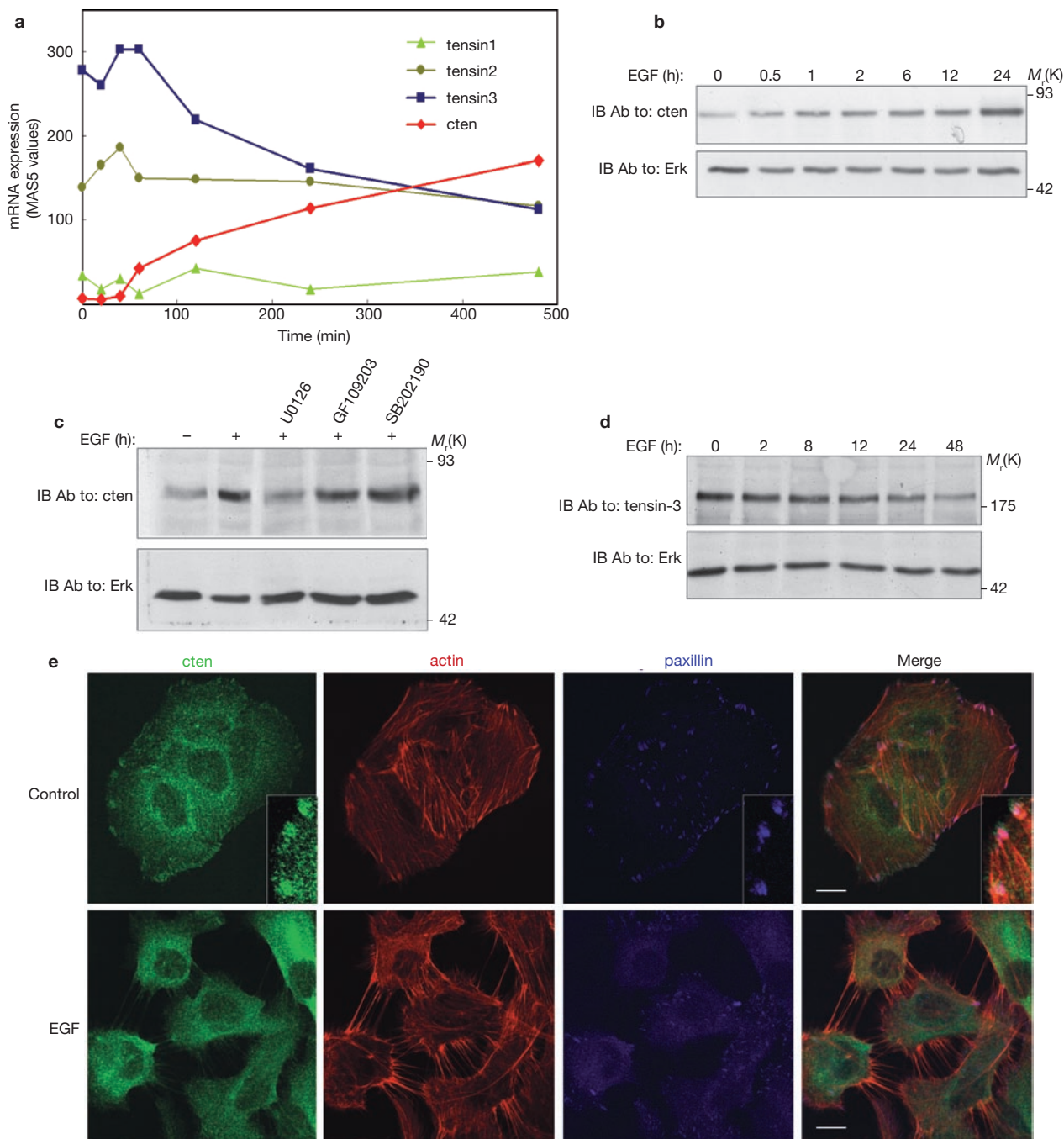


**Figure 1** EGF-induced downregulation of tensin-3, along with upregulation and reorganization of cten. **(a)** HeLa cells were stimulated with epidermal growth factor (EGF; 20 ng ml<sup>-1</sup>) for the indicated time intervals and RNA was analysed using oligonucleotide arrays. MAS5 expression values of the four tensin family members, at the indicated time points, are presented. **(b)** Serum-starved MCF10A cells were treated without or with EGF for the indicated time intervals. Cells were then lysed and subjected to immunoblot (IB) analysis. Ab, antibody; K, relative molecular mass in thousands. **(c)** Serum-starved MCF10A cells were incubated for 12 h with EGF (10 ng ml<sup>-1</sup>) containing minimal medium supplemented without or with the following inhibitors: U0126 (5  $\mu$ M; a Mek inhibitor), GF109203 (3  $\mu$ M; a protein kinase C inhibitor) and

SB202190 (10  $\mu$ M; a p38 inhibitor). For control, cells were incubated without the addition of EGF (-). **(d)** MCF10A cells were treated as in **b**. An anti-tensin-3, or an anti-Erk antibody, were used for immunoblotting. Uncropped images of the blots shown in **b** and **c** are presented in Supplementary Information, Fig. S4. **(e)** Serum-starved MCF10A cells were incubated without (Control) or with EGF for 24 h. Thereafter, immunofluorescence analysis was performed using a rabbit anti-cten antibody (green), TRITC-conjugated phalloidin (red) and a mouse anti-paxillin monoclonal antibody (blue). An overlay of the three fluorescent signals, generating white colour in areas of colocalization, is shown in the right column. Enlargement of plasma membrane regions are presented in the inner boxes. Scale bars, 10  $\mu$ m.

autocrine EGFR activation (see Supplementary Information, Fig. S1d). In conclusion, these results raise the possibility that reciprocal regulation of cten and tensin-3 plays a general role in cell adhesion and migration.

The normal human mammary cell line, MCF10A, has been characterized as a cellular model for EGF-induced migration regulated by the Erk/MAPK cascade<sup>13</sup>. We observed that migration of MCF10A cells through

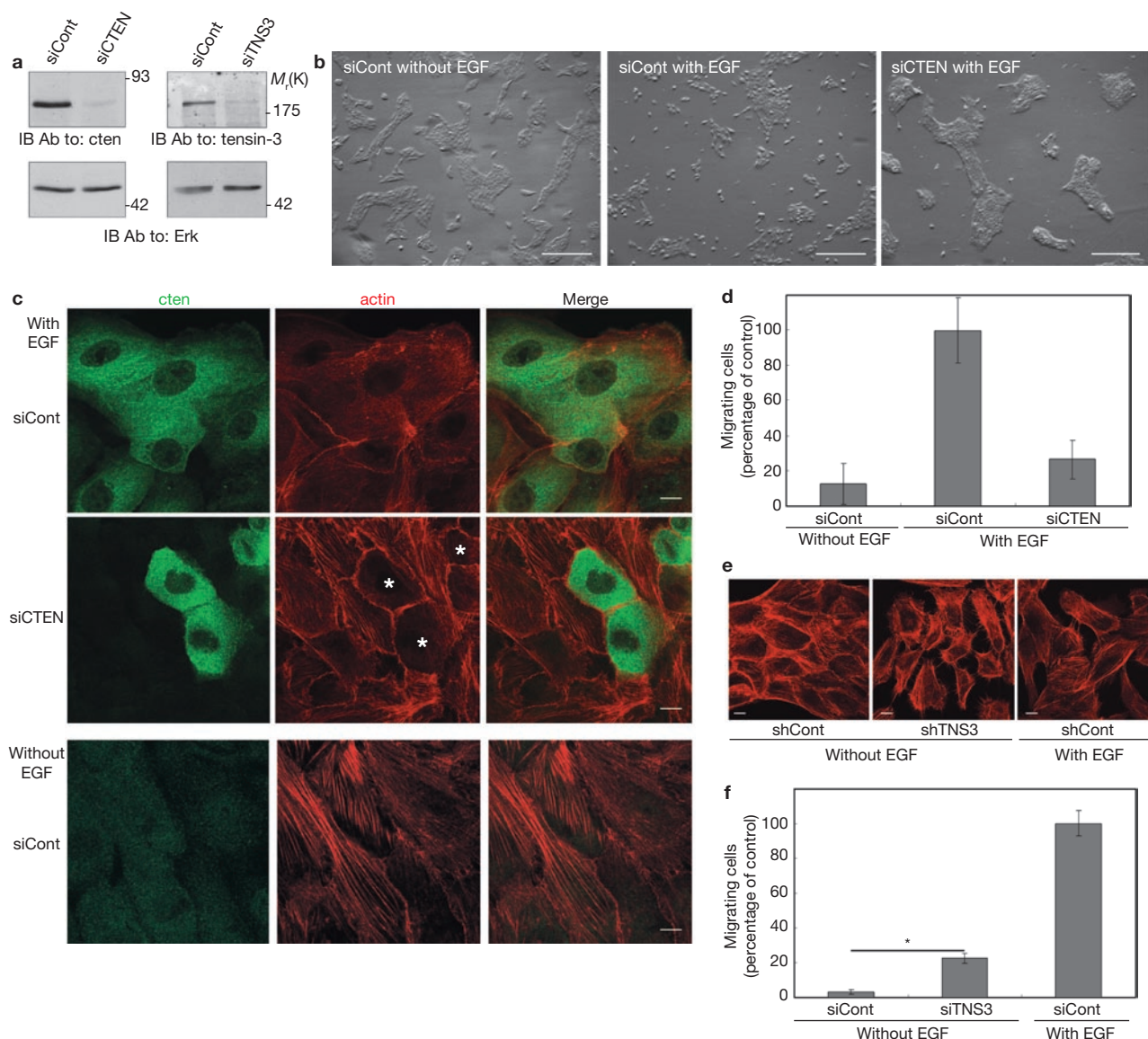


**Figure 2** Mammary cell migration is inhibited following knockdown of cten and increased following tensin-3 knockdown. (a) MCF10A cells were transfected with small interfering RNA (siRNA) oligonucleotides directed to cten (siCTEN), control siRNA oligonucleotides (siCont) or siRNA oligonucleotides directed to tensin-3 (siTNS3), and incubated in serum-containing full medium, with (left panel) or without epidermal growth factor (EGF; right panel). Thereafter, whole cell extracts were prepared and subjected to immunoblot (IB) analysis. Uncropped images of blots are shown in Supplementary Information, Fig. S4. K, relative molecular mass in thousands. (b) MCF10A cells were transfected with the indicated siRNA oligonucleotides and then incubated for 48 h in serum-containing medium, without or with EGF. Images were obtained using a digital camera. Scale bars, 500  $\mu$ m. (c) MCF10A cells were transfected with the indicated siRNA oligonucleotides and grown in full medium containing EGF (top two rows), or lacking EGF (bottom row), prior to

Transwell membranes is dependent on the presence of EGF in the growth medium, whereas serum factors are insufficient for migration induction (see Supplementary Information, Fig. S2a). Similarly to the observations made in HeLa cells, treatment of MCF10A cells with EGF resulted in induction of cten and reduction in tensin-3 levels (Fig. 1b, d). Because a Mek inhibitor (U0126) completely blocked cten induction, but inhibition of either protein kinase C (with GF109203) or p38 (using SB202190)

immunofluorescence analysis. The fluorescent signals of cten (green) and actin (red) are shown, along with an overlay (Merge, right column). Scale bars, 10  $\mu$ m. Asterisks mark cells that did not express siCTEN. (d) MCF10A cells transfected with the indicated siRNA oligonucleotides were incubated in Transwell chambers in serum-containing medium, without or with EGF, and their migration measured and normalized to cells transfected with control siRNA. Shown are mean  $\pm$  s.d.; bars,  $n = 12$ ). (e) MCF10A cells were infected with short hairpin RNA (shRNA)-tensin-3 or with shRNA-control lentiviruses. Thereafter, cells that stably incorporated the shRNA were selected with puromycin, and grown in serum-containing medium, without or with EGF, prior to fixation and staining with TRITC-phalloidin. Scale bars, 10  $\mu$ m. (f) MCF10A cells transfected with the indicated siRNA oligonucleotides were plated in Transwell plates containing full medium without or with EGF. Cell migration was quantified 24 h later as in d. Shown are mean  $\pm$  s.d.; asterisk indicates  $P < 0.005$ , Student's  $t$ -test,  $n = 5$ ).

was ineffective (Fig. 1c), we concluded that Erk activity is essential for the induction of cten by EGF. The necessity of Erk activation suggests that the reported Erk/MAPK-driven migration of MCF10A cells<sup>13</sup> may depend on the induction of regulatory proteins such as cten.

In agreement with previous immunolocalization studies<sup>6</sup>, we localized cten of resting cells to paxillin-containing focal adhesion sites (Fig. 1e). Remarkably, along with EGF-induced cten expression and dissociation

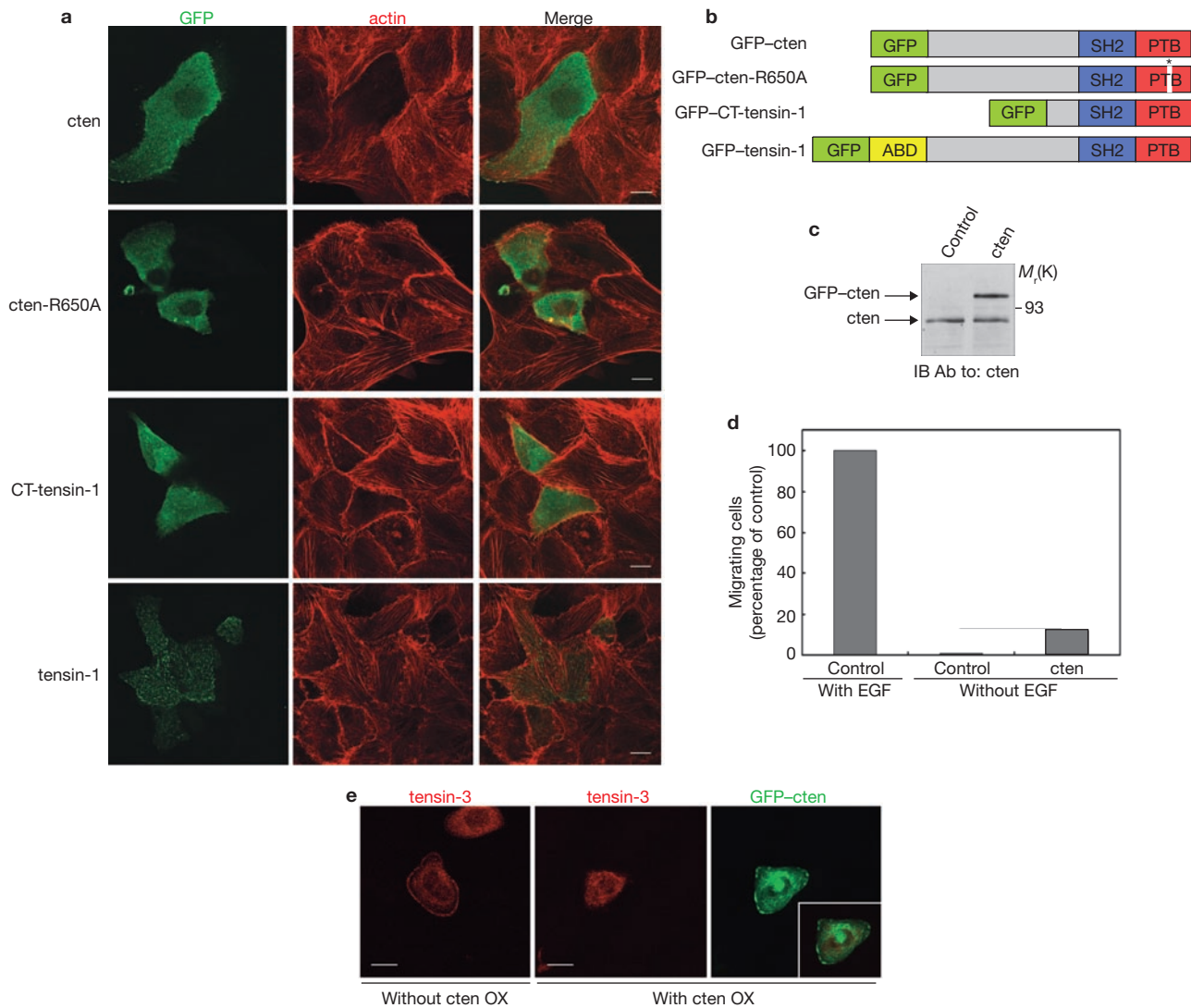


**Figure 3** Cten expression disrupts actin stress fibre organization, induces cell migration and displaces tensin-3 from focal adhesions. **(a)** MCF10A cells expressing the indicated green fluorescent protein (GFP) fusion proteins were immunostained with TRITC-phalloidin. The fluorescent signals of GFP (green) and actin (red) are shown, along with a merge column (right). Scale bars, 10  $\mu$ m. **(b)** A schematic representation of GFP fusion constructs of cten, cten mutated in the PTB domain (R650A; arginine 650 replaced by an alanine), tensin-1 and the carboxyl terminus of tensin-1 (ABD, actin-binding domain). **(c)** MCF10A cells were infected with a lentivirus encoding for GFP-cten, or with an empty control virus. Stably infected cells were selected with blastocidin. Following drug selection, cell lysates were prepared and subjected

to immunoblot (IB) analysis using an anti-cten polyclonal antibody. Arrows indicate the endogenous cten and the ectopic GFP-cten. Uncropped images of blots are shown in Supplementary Information Fig. S4. K, relative molecular mass in thousands. **(d)** GFP-cten-expressing MCF10A cells, or control cells, were plated in Transwell chambers in serum-containing medium, without epidermal growth factor (EGF), and their migration measured and normalized to EGF-treated control cells. Shown are mean values ( $n = 2$ ). **(e)** MCF10A cells ectopically overexpressing (OX) GFP-cten, or control cells, were grown in the absence of EGF and stained for tensin-3. The micrographs present locations of GFP (green), tensin-3 (red) or both (yellow; inset). Note the near absence of colocalization of cten and tensin-3. Scale bars, 10  $\mu$ m.

of cellular colonies (Fig. 1e; induction is not apparent due to normalization of the immunofluorescence signal), cten localization was no longer restricted to focal adhesion sites of stimulated cells. We assume that the induction and redistribution of cten overrides the staining signal of adhesion sites. Indeed, biochemical analysis confirmed an EGF-induced enrichment of cten in both the detergent-soluble and the detergent-insoluble fraction; the latter is known to include actin-associated proteins (see Supplementary Information, Fig. S2b). In parallel, actin stress fibres, which are normally anchored at paxillin-containing focal adhesion sites, disintegrated following EGF treatment and reorganized in cortical bundles (Fig. 1e; lower row). Accordingly, in resting cells, tensin-3 is detergent-insoluble and localizes in cell-matrix adhesions, but it largely

disappears following EGF stimulation (see Supplementary Information, Fig. S2b, c). These results indicate that EGF-induced upregulation of cten and downregulation of tensin-3 correlate with actin fibre remodeling, which may assist cell spreading.

To address the dependence of EGF-induced cell migration on the levels of cten and tensin-3, we depleted endogenous cten and tensin-3 using specific short interfering RNA (siRNA; Fig. 2a). In the absence of EGF, MCF10A cells form dense cell clusters, whereas EGF treatment induces cell scattering (Fig. 2b). In contrast, following depletion of cten, EGF-stimulated cells presented large, densely packed colonies, which resemble the morphology of cells grown in the absence of EGF. Fluorescent labelling revealed that depletion of cten resulted in

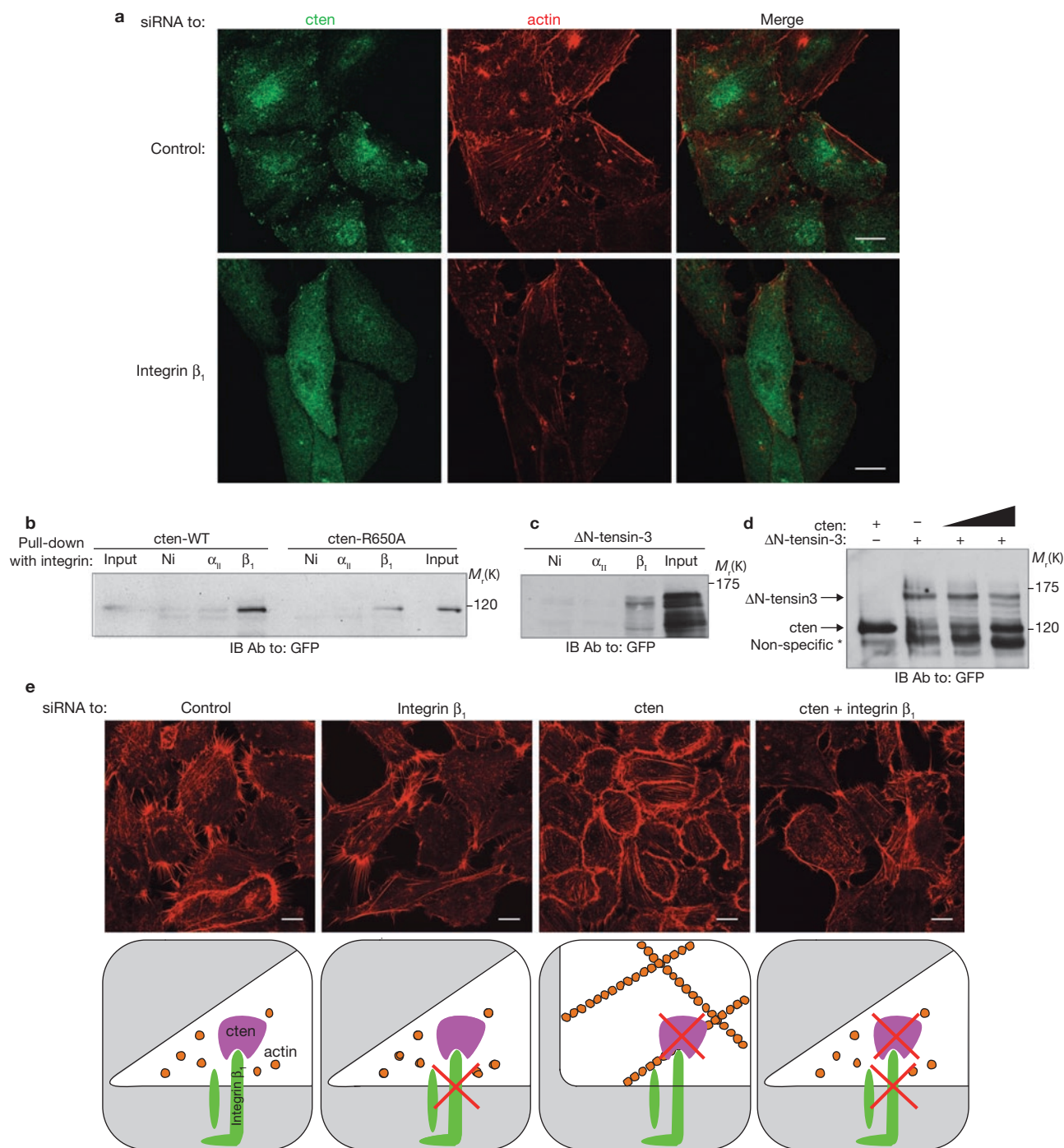


**Figure 4** Cten displaces tensin-3 from the tail of integrin  $\beta_1$ . **(a)** MCF10A cells transfected with the indicated small interfering RNA (siRNA) oligonucleotides were grown in serum-containing medium, without epidermal growth factor (EGF), prior to fixation and staining with a rabbit anti-cten antibody (green) and TRITC-phalloidin (red). An overlay of the two signals is shown in the right column (Merge). Scale bars, 10  $\mu$ m. **(b)** Lysates of HEK-293T cells ectopically expressing a green fluorescent protein (GFP) fused to the indicated cten proteins were subjected to a pull-down assay using immobilized forms of integrin  $\alpha_{II}$  or  $\beta_1$  carboxyl-terminal tails. Bound proteins, as well as input mixtures (5%), were resolved by electrophoresis and detected using an anti-GFP antibody. Ni indicates proteins adsorbed to naked nickel beads. IB, immunoblot; K, relative molecular mass in thousands; WT, wild type. **(c)** Lysates of HEK-293T cells ectopically expressing a GFP protein fused

to tensin-3 lacking the amino-terminal actin-binding domain ( $\Delta$ N-tensin-3) were treated as in **b**. **(d)** An immobilized carboxy-terminal tail of integrin  $\beta_1$  was incubated with a mixture of lysates derived from HEK-293T cells transiently expressing either GFP- $\Delta$ N-tensin-3 or GFP-cten (increasing amounts). Tightly associated proteins were resolved by electrophoresis and detected using an anti-GFP antibody. An asterisk indicates a non-specific protein band. Uncropped images of blots are presented in Supplementary Information, Fig. S4. **(e)** MCF10A cells transfected with the indicated siRNA oligonucleotides, either alone or in combination, were grown in serum-containing medium with EGF, prior to fixation and staining with TRITC-phalloidin. Scale bars, 10  $\mu$ m. The lower row presents schematics showing actin (orange beads) redistribution in response to knockdown (represented by X) of integrin  $\beta_1$  (green), cten (purple) or both.

**Table 1.** Correlation in breast cancer patients between cten expression and disease parameters

Cten correlation to:	Spearman rank correlation (Rho)	P value
EGFR	0.785	0.0006*
HER2/ErbB-2	0.67	0.004*
Oestrogen receptor	-0.48	0.004*
Lymph-node metastasis (number of lymph nodes: 0, 1–3, >3)	0.47	0.001*
Histological grade (I, II, III)	0.47	0.001*
Tumour size	0.01	0.84

The numbers were calculated on the basis of analyses performed using 272 samples derived from invasive breast tumours. Spearman's rank correlation test was used to determine the correlations. A False Discovery Rate test was used to correct the alpha value for multiple comparisons. Asterisks indicate statistically significant correlations. EGFR, epidermal growth factor receptor.

restoration of a dense network of actin fibres, despite the presence of EGF in the growth medium (Fig. 2c). On the other hand, stress fibres were not observed in neighbouring cells that retained cten expression (cells marked with asterisks) or in EGF-treated cells that had been transfected with control oligonucleotides (siCont; Fig. 2c). Moreover, depletion of cten caused a 70% reduction in cell migration (Fig. 2d). In conclusion, EGF-driven cell movement is dependent on the induction of cten and associates with reorganization of the actin cytoskeleton.

Apart from inducing expression of cten, EGF drives a reduction in the expression of tensin-3. Cells in which tensin-3 was stably depleted displayed colony scattering and actin stress fibre disintegration, even in the absence of EGF (Fig. 2e). In addition, under these conditions, tensin-3 depletion was sufficient to promote partial cell migration (23% of the EGF signal; Fig. 2f). Conceivably, downregulation of tensin-3 complements EGF-induced upregulation of cten, and together they instigate reorganization of the actin cytoskeleton and cell motility.

To resolve the relationships between cten expression and actin stress fibres, we fused green fluorescent protein (GFP) to full-length cten. Ectopic expression of GFP-cten in unstimulated MCF10A cells caused extensive disassembly of stress fibres in 60% of GFP-cten-expressing cells ( $n = 28$ ; Fig. 3a). Moreover, ectopic expression of the fusion protein (schematically presented in Fig. 3b) reproducibly enhanced sub-maximal cell migration in the absence of EGF (Fig. 3c, d). Notably, actin stress fibres are stabilized by interactions with integrin-centred focal adhesion sites<sup>14</sup>, a process in which tensins have been implicated<sup>5</sup>. Indeed, upregulation of tensin induces the formation of stress fibres<sup>15</sup>, whereas cleavage of tensin by caspase-3 induces disintegration of stress fibres<sup>16</sup>. Structurally, cten resembles a truncated form of tensin, which lacks the actin-binding domain<sup>6</sup>. Hence, we speculated that cten acts as a competitive inhibitor, which blocks binding of PTB-containing proteins to integrins. In line with this proposition, overexpression of a truncated cten lacking the PTB domain (data not shown) or a point mutant unable to bind integrins (R650A; see below and Fig. 3a) did not significantly affect actin organization. Moreover, similar to the effect of cten, ectopic expression of a truncated mutant form of tensin-1 lacking the actin-binding domain (Fig. 3b; GFP-CT-tensin-1) resulted in disassembly of the actin stress fibres in 75% of GFP-CT-tensin-1-expressing cells ( $n = 24$ ), whereas overexpression of full-length tensin-1 exerted no significant effect (Fig. 3a). In conclusion, the ability of cten to disassemble actin stress fibres is mediated by its PTB domain, which probably competes with tensin-3 for the cytoplasmic tail of integrins. Indeed, forced upregulation of cten can displace tensin-3 from focal adhesion sites of unstimulated cells (Fig. 3e).

These results indicate that cten regulates the integrity of stress fibres, as well as cell migration, by binding to integrins. Integrins  $\beta_1$ ,  $\beta_4$  and  $\beta_8$  are highly expressed in MCF10A cells (data not shown), but

analyses using blocking antibodies or siRNAs identified integrin  $\beta_1$  as the subtype most relevant to both adhesion and migration of MCF10A cells (see Supplementary Information, Fig. S3a, b). Indeed, depletion of integrin  $\beta_1$  resulted in complete loss of stress fibres, whereas depletion of integrin  $\beta_8$ , an isoform involved only in cell migration, exerted no effect (see Supplementary Information, Fig. S3c). Conceivably, following induction by EGF, cten blocks the binding of PTB-containing, actin-binding proteins (such as tensin-3) to the tail of integrin  $\beta_1$ , thereby disintegrating stress fibres. In line with this model, cten colocalizes with integrin  $\beta_1$  in cell-matrix adhesions (see Supplementary Information, Fig. S3d), but cten dissociates from these sites when integrin  $\beta_1$  is depleted (Fig. 4a). The ability of both cten and a soluble form of tensin-3 ( $\Delta N$ -tensin-3) to bind to the cytoplasmic tail of integrin  $\beta_1$  was confirmed by using *in vitro* assays (Fig. 4b, c). Similarly, these analyses established competitive relationships between cten and tensin-3 for binding to the tail of integrin  $\beta_1$  (Fig. 4d). To verify the role of the PTB domain of cten, we superimposed the predicted structure on the published crystal structure of the PTB domain of talin<sup>17</sup>. This analysis identified arginine 650 of cten as an integrin interfacing residue (data not shown). As expected, the point mutant R650A-cten almost completely lost the ability to bind with the cytoplasmic tail of integrin  $\beta_1$  (Fig. 4b).

Retention of stress fibres by cten-depleted EGF-stimulated cells (Fig. 2c) may reflect recruitment of PTB-containing, actin-binding proteins (for example, tensins) to the tail of integrin  $\beta_1$ , as it is no longer capped by cten. To examine this model, we simultaneously knocked-down cten and integrin  $\beta_1$  in MCF10A cells, which we then stimulated with EGF. The double knockdown completely reversed the effect of the single knockdown of cten (Fig. 4e). Moreover, the resulting phenotype was strikingly similar to the phenotype of integrin- $\beta_1$ -depleted cells. Notably, a similar double knockdown of integrin  $\beta_8$  and cten yielded no comparable effects (data not shown). Thus, the phenotypic dominance of integrin  $\beta_1$  depletion strongly identifies this adhesion molecule as a functional partner of cten, in line with a 'tensin-cten switch' model.

Aberrant expression and activation of EGFR are richly implicated in breast cancer progression<sup>17</sup>. To address the potential roles of cten in cancer, we generated a monoclonal antibody to human cten and immunohistochemically analysed a set of 272 paraffin-embedded samples of invasive breast carcinomas. The results are summarized in Table 1. Interestingly, whereas statistical analysis found no correlation between cten expression and size of primary tumours, the data indicated a significant correlation with high expression of EGFR and HER2, as well as a strong correlation with the absence of the oestrogen receptor. Perhaps most important are the statistically significant correlations that we observed between cten positivity and both high tumour grade ( $P < 0.001$ ) and the ability to

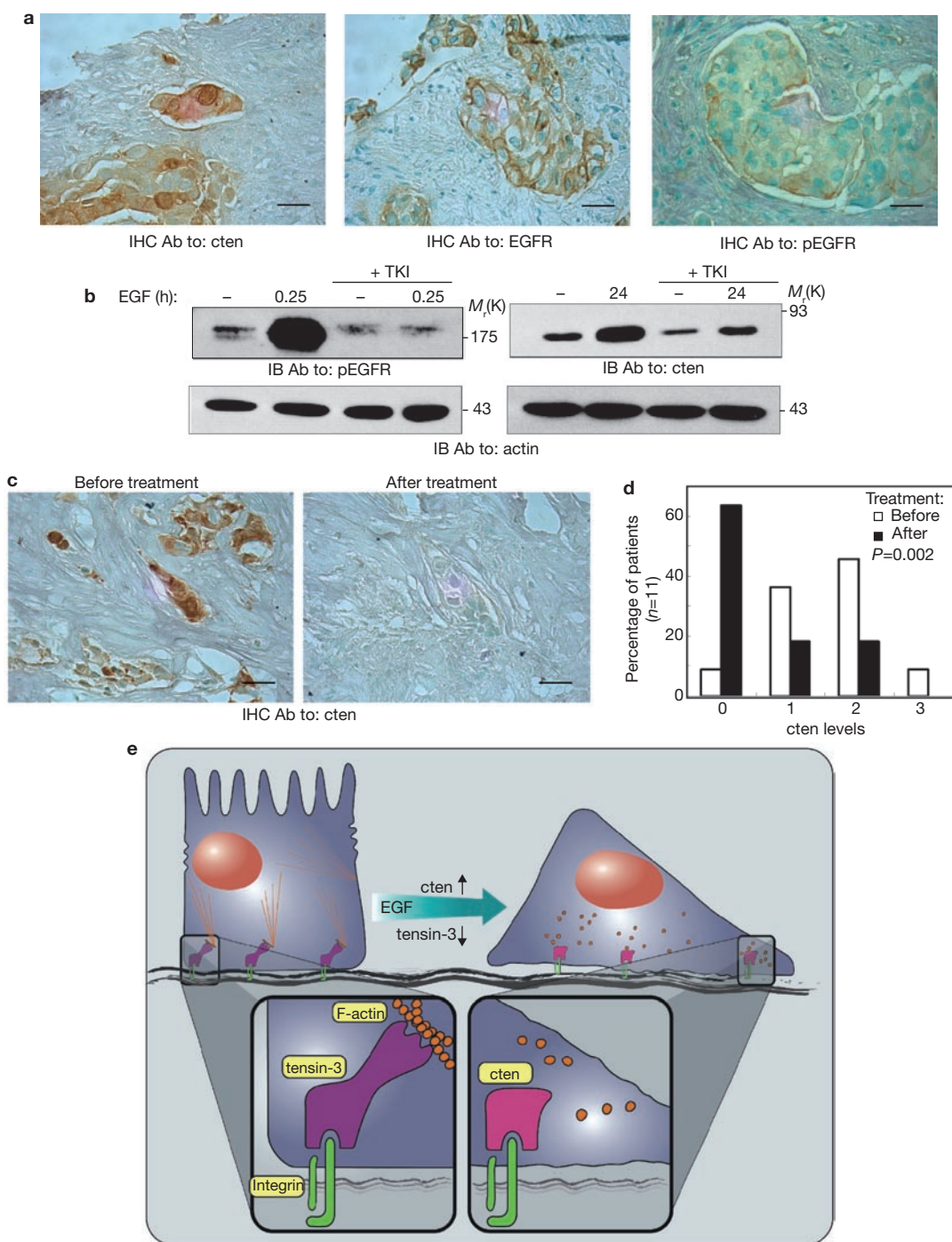


**Figure 5** Cten expression in mammary tumours associates with EGFR activation, and undergoes downregulation in patients treated with an EGFR-specific kinase inhibitor. **(a)** Thin sections of a paraffin-embedded inflammatory breast carcinoma tumour were immunostained using an anti-cten monoclonal antibody (left panel), an anti-EGFR (epidermal growth factor receptor) antibody (middle panel) or an anti-phosphorylated EGFR (tyrosine-1068) antibody (right panel). Regions positive for cten, EGFR or phospho-EGFR appear in brown, whereas nuclei stained with Methyl Green appear in dark green. Scale bars, 15  $\mu$ m. IHC Ab, immunohistochemistry antibody. **(b)** AU-565 human mammary cancer cells were pre-treated with or without a tyrosine kinase inhibitor (TKI; GW-2974, 25  $\mu$ M) for 1 h followed by stimulation with EGF (100 ng ml<sup>-1</sup>) for 15 min. Alternatively, cells were treated with EGF (10 ng ml<sup>-1</sup>) for 24 h in the absence or presence of GW-2974 (1  $\mu$ M). Thereafter, cell extracts were subjected to immunoblotting with the indicated antibodies. K, relative molecular mass in thousands.

**(c)** Immunohistochemical analysis of cten in an inflammatory breast tumour obtained from a patient before and after a 3-week-long treatment with lapatinib (Tykerb). Scale bars, 15  $\mu$ m. Note the tumour emboli in the lymphovascular area and reduction in cten expression (from score 2 to score 0). **(d)** Statistical analysis of cten expression levels in patients scored (0–3) by immunohistochemistry before and after TKI treatment ( $n = 11$ ,  $P < 0.002$ ; paired  $t$ -test). **(e)** A model representing the functions of cten and tensin-3 in promoting EGF-induced cell migration. Resting cells, which are packed in an epithelial layer, contain stress fibres anchored to focal adhesion sites through tensin-3, or other actin binders simultaneously binding actin filaments and integrin (through a PTB domain). Following EGF stimulation, tensin-3 expression is downregulated and cten is upregulated, to a level that is sufficient for displacement of tensin-3 from integrin. Consequently, tensin-3 dissociates from focal adhesion sites, leading to the breakdown of actin stress fibres and initiation of cell migration.

metastasize to nearby lymph nodes ( $P < 0.001$ ). In conclusion, these data implicate cten in breast cancer progression and identify it as a potential marker of a poorly differentiated, relatively aggressive sub-population of invasive breast tumours, which are driven by EGFR/HER2 signalling.

Inflammatory breast cancer (IBC) is an example of a highly aggressive form of mammary cancer<sup>18</sup>; IBC often overexpresses HER2 and manifests a large degree of lymphovascular invasion<sup>19</sup>. Using a small cohort of HER2-positive IBC patients ( $n = 18$ ), we detected high cten expression in 56% of tumour biopsies (see an example in Fig. 5a). In addition, we found a strong correlation between EGFR activation (phospho-EGFR) and cten expression ( $P < 0.0001$ ; see Supplementary Information, Table S1). This association was supported by *in vitro* treatment of cultured IBC cells, AU-565, with a selective dual EGFR/HER2 tyrosine kinase inhibitor (TKI; GW-2974; Fig. 5b). Furthermore, because a structurally related dual-specificity TKI, lapatinib (Tykerb), is currently being tested in clinical trials, we examined the effect on cten in sequential IBC biopsies obtained prior to and during lapatinib monotherapy. Representative immunohistochemical analyses of tumour biopsies from the same patient, before and after a 21-day treatment with the drug, are presented in Fig. 5c. Similar analyses performed on biopsies obtained from all phospho-EGFR positive inflammatory breast tumours derived from the small cohort of patients revealed statistically significant downregulation of cten expression in most tumours (Fig. 5d;  $P < 0.002$ ). These observations are in line with the previously reported reduction in pEGFR, pHER2 and pErk following lapatinib treatment<sup>20,21</sup>. We conclude that cten expression in breast cancer is highly dependent on EGFR activation, and may predict the response to EGFR/HER2-targeted therapy.

The transition of an epithelial sheet into motile cells is a complex process, involving disassembly of actin stress fibres and cell–cell adhesion sites<sup>2,22</sup>. Our findings propose that EGF regulates actin remodelling by the following mechanism (see Fig. 5e). In resting mammary epithelial tissues, the polarized cell structure is maintained by actin stress fibres that are stabilized by integrin-based focal adhesion sites<sup>14</sup>. This stabilization is mediated by tensin-3, which simultaneously interacts with actin fibres and with the cytoplasmic tail of integrin  $\beta_1$  (ref. 5). Hence, dissociation of the integrin–tensin–actin complex is expected to disintegrate stress fibres. To ensure effective dissociation, EGF activates two complementary processes: tensin-3 levels are reduced, whereas cten levels are concomitantly upregulated, thereby capping the tail of integrin. Interestingly, dynamic associations of tensins with focal adhesion sites were observed in fibroblasts<sup>23</sup> but, in other cells, talin, which also links integrins to actin fibres, may play a role that is analogous to the function of tensin<sup>24</sup>. Growth-factor-induced cell migration involves not only disruption of cell-to-matrix interactions, through the ‘tensin–cten switch’ we report herein, but also weakening of cell-to-cell adhesion. For example, a molecular switch has been described whereupon, during cell migration, the epithelial cadherin (E-cadherin) is replaced by the mesenchymal cadherin (N-cadherin)<sup>25</sup>.

The transformation of epithelial sheets into invasive carcinomas critically depends on re-organization of the actin cytoskeleton<sup>26</sup>. Our results indicate that upregulation of cten contributes to actin reorganization and, eventually, to mammary tumour invasion (Table 1). Dynamic changes in cten expression may not be restricted to mammary carcinoma progression; cten is also upregulated in thymomas and in lung cancers<sup>27,28</sup>, but in prostate cancers it is downregulated<sup>6</sup>. The association in mammary tumours between cten expression and active EGFR

(Fig. 5a), as well as the observed reduction in cten expression in lapatinib-treated patients (Fig. 5c, d), suggests that the ‘tensin–cten switch’ that we uncovered serves as a marker for EGFR-driven tumours, as well as a component of a protein signature that is capable of predicting patient response to EGFR-targeted therapy. Future studies will address the prognostic and predictive significance of the ‘tensin–cten switch’ in cancer progression. □

## METHODS

**Reagents and antibodies.** Unless indicated, materials were purchased from Sigma (St Louis, MO), antibodies from Santa Cruz Biotechnology (Santa Cruz, CA) and kinase inhibitors from Calbiochem (San Diego, CA). An anti-cten monoclonal antibody was generated by immunizing mice with a GST–cten fusion protein (amino acids 181–353). Polyclonal antibodies to cten and tensin-3 have been described previously<sup>29</sup>. A rabbit polyclonal antibody directed to EGFR phosphorylated at tyrosine 1068 was purchased from Cell Signaling (Beverly, MA). The following siRNA oligonucleotides were obtained from Invitrogen (Groningen, The Netherlands): siCTEN-I, UUCUCAUUGACAUGGUGCUCUGGGC; siCTEN-II, GGAGGAAUCUGAAGCCUUGGACAU; siCont, CCCGUAUACGACACC GAGUAGUCUU. The accession numbers of SMARTpool siRNA oligonucleotides (Dharmacon, Lafayette, CO) were as follows: tensin-3: MQ-009997-00; integrin  $\beta_1$ : MQ-004506-00; and integrin  $\beta_8$ : MQ-008014-01. The following sequence was used to construct short hairpin RNA (shRNA)-tensin-3: CCGGCGTGTGTAC TTGAACTCTGTCTCGAGACAGAGTTCAAGTACCACACGTTT.

**Expression vectors.** Full-length cten cDNA was assembled in an expression vector using two-way PCR, in which we amplified the 3’ part of the coding region using a cDNA clone from the RZPD library (RZPD, Berlin, Germany; clone no. IRAUp969B0180D) as template, and the 5’ part was amplified from a previously described cten plasmid<sup>6</sup>. Expression vectors encoding full-length tensin-1 and CT-tensin-1 were kindly provided by Kenneth Yamada (National Institutes of Health, Bethesda, MD) and Shin Lin (University of California at Irvine, Irvine, CA). shRNA lentiviral plasmids directed at tensin-3 were purchased from Sigma. Bacterial expression vectors for His-tagged integrins were a generous gift from Mark Ginsberg (Scripps Research Institute, La Jolla, CA). GFP–cten was cloned into the ViraPower lentiviral-based expression system of Invitrogen.

**Cell lines and transfection.** MCF10A cells were grown in DMEM:F12 (1:1) medium supplemented with antibiotics, EGF (10 ng ml<sup>-1</sup>), insulin (10  $\mu$ g ml<sup>-1</sup>), cholera toxin (1  $\mu$ g ml<sup>-1</sup>), hydrocortisone (1  $\mu$ g ml<sup>-1</sup>) and heat-inactivated horse serum (5%). Cells were transfected using jet-PEI (PolyPlus-Transfection; Illkirch, France). Alternatively, cells were transfected with siRNA oligonucleotides using Oligofectamine (Gibco BRL; Grand Island, NY).

**Lysate preparation and immunoblotting analysis.** Cells were washed briefly with ice-cold saline, and scraped in a buffered detergent solution (25 mM HEPES (pH 7.5), 150 mM NaCl, 0.5% Na-deoxycholate, 1% NP-40, 0.1% SDS, 1 mM EDTA, 1 mM EGTA, 0.2 mM Na<sub>3</sub>VO<sub>4</sub> and a protease inhibitor cocktail diluted at 1:1000). For equal gel loading, protein concentrations were determined by using the Bradford technique. Following gel electrophoresis, proteins were electrophoretically transferred to a nitrocellulose membrane. Membranes were blocked in TBST buffer (0.02 M Tris-HCl (pH 7.5), 0.15 M NaCl and 0.05% Tween 20) containing 10% low-fat milk, blotted with a primary antibody for 1 h, washed with TBST and incubated for 30 min with a secondary antibody linked to horseradish peroxidase.

**Immunofluorescence.** Cells were treated and labelled for immunofluorescence as described previously<sup>23</sup>. Confocal microscopy was performed using a Nikon eclipse TE300 microscope (Oberkochen, Germany).

**Transwell cell migration assay.** MCF10A cells ( $4 \times 10^5$  cells per well) were plated in the upper compartment of a 24-well Transwell tray (Corning, Acton, MA) in full medium lacking EGF. The lower compartment contained the indicated medium, and cells were allowed to migrate through the intervening nitrocellulose membrane (8  $\mu$ m pore size) during 16 h of incubation at 37 °C. The filter was then removed, fixed for 15 min in phosphate-buffered saline (PBS) containing

paraformaldehyde (3%), followed by cell permeabilization in Triton X-100 (0.05%, in PBS) and stained with methyl violet. Cells growing on the upper side of the filter were scraped using cotton swabs, whereas cells growing on the bottom side of the filter were photographed and counted. Alternatively, stained membranes were lysed in 10% acetic acid, and their signal measured using a spectrophotometer.

**RNA preparation and oligonucleotide microarray hybridization.** Cells were lysed, and RNA purified using a Versagene kit (Gentra Systems, Minneapolis, MN). RNA (10 µg) was labelled, fragmented and hybridized to an Affymetrix HG-U133A oligonucleotide arrays (Affymetrix Incorporated, Santa Clara, CA). Arrays were scanned using a laser confocal scanner, and the expression value for each gene was calculated using Affymetrix Microarray Software v.5.0 (MAS5). The complete microarray data sets are available from the Gene Expression Omnibus (GSE6786).

**Integrin binding assay.** Poly-histidine-tagged carboxyl tails of integrins ( $\alpha_{IIb}$ ,  $\beta_1$ ) immobilized on Nickel beads have been described previously<sup>30</sup>. Immobilized proteins were incubated for 1 h at 4 °C with cleared extracts of transfected HEK293T cells. The beads were then extensively washed with imidazole-containing washing solution (50 mM NaH<sub>2</sub>PO<sub>4</sub> (pH 8), 300 mM NaCl, 20 mM imidazole and 0.1% Triton X-100). For competition assays, beads coated with integrin  $\beta_1$  were incubated with lysates of cells expressing GFP- $\Delta$ N-tensin-3, along with increasing volumes of lysates of cells expressing GFP-cten. To equal the total amount of GFP fusion proteins in each reaction, lysates of GFP-expressing cells were respectively added to the reactions.

**Immunohistochemical analysis.** Two tumour collections were used in this study; one contains formalin-fixed, paraffin-embedded tissues of 362 invasive breast carcinomas that were retrieved from the histopathology files of IPATIMUP and Hospital de São João, Porto, Portugal. Relevant data were available for 272 of the 362 cases. The second collection is of IBC patients in which tumour biopsies were collected prior to initiating lapatinib therapy as part of a clinical trial in which patients with recurrent IBC were treated with lapatinib (1,500 mg d<sup>-1</sup>). The trial has been conducted in accordance with the 1996 version of the Declaration of Helsinki. The study protocol was approved by Institutional Review Boards and all patients provided a signed informed consent. Antigen retrieval was performed by using either an ethylenediaminetetraacetic solution at pH 9.0, at 98 °C for 20 min or 0.1 M citrate buffer at pH 6.0 (DakoCytomation, Carpinteria, CA, USA). After immunostaining, slides were counterstained with Mayer's haematoxylin or with 4% methyl green. Protein expressions on slides were independently scored by at least two pathologists.

**Statistical analysis.** All analyses were performed using SPSS 13.0. First, means and standard deviations of the continuous variables and frequencies of the categorical variables were obtained. Then, the Chi-Square test and the Spearman's correlation rank for non-parametric variables were used to assess the relationships between the categorical variables. Paired *t*-test was used to assess the difference from 'before' to 'after' treatment in the continuous variables (cten expression levels). All statistical tests used a two-tailed significance level of *P* < 0.05. When multiple comparisons were made, a False Discovery Rate test was used to correct the alpha value.

*Note: Supplementary Information is available on the Nature Cell Biology website.*

#### ACKNOWLEDGEMENTS

We thank Kenneth Yamada, Shin Lin and Mark Ginsberg for plasmids; Dalia Seger and Hadassa Degani for guidance with xenografts; Miriam Eisenstein for structure prediction; and Benjamin Geiger and Alexander Bershadsky for critical comments. Our laboratory is supported by research grants from the Israel Cancer Research Fund, the German Israel Foundation, the Prostate Cancer Foundation, the European Commission and the National Cancer Institute (grants CA72981 and CA102537). Y.Y. is the incumbent of the Harold and Zeldia Goldenberg Professorial Chair. T.S. was supported in part by the Ridgefield Foundation, the Israel Science Fund and the European Commission (EC FP6). S.C. is the recipient of a grant from Fundação para Ciência e Tecnologia (FCT), Lisboa, Portugal.

#### COMPETING FINANCIAL INTERESTS

The authors declare no competing financial interests.

Published online at <http://www.nature.com/naturecellbiology/>  
Reprints and permissions information is available online at <http://npg.nature.com/reprintsandpermissions/>

- Wells, A., Kassis, J., Solava, J., Turner, T. & Lauffenburger, D. A. Growth factor-induced cell motility in tumor invasion. *Acta Oncol.* **41**, 124–130 (2002).
- Ridley, A. J. *et al.* Cell migration: integrating signals from front to back. *Science* **302**, 1704–1709 (2003).
- Bauer, J. *et al.* *In vitro* model of angiogenesis using a human endothelium-derived permanent cell line: contributions of induced gene expression, G-proteins, and integrins. *J. Cell Physiol.* **153**, 437–449 (1992).
- Gordon, S. R. & Staley, C. A. Role of the cytoskeleton during injury-induced cell migration in corneal endothelium. *Cell Motil. Cytoskeleton* **16**, 47–57 (1990).
- Lo, S. H. & Tensin. *Int. J. Biochem. Cell Biol.* **36**, 31–34 (2004).
- Lo, S. H. & Lo, T. B. Cten, a COOH-terminal tensin-like protein with prostate restricted expression, is down-regulated in prostate cancer. *Cancer Res.* **62**, 4217–4221 (2002).
- Yarden, Y. & Sliwkowski, M. X. Untangling the ErbB signalling network. *Nature Rev. Mol. Cell Biol.* **2**, 127–137 (2001).
- Ridley, A. J. & Hall, A. The small GTP-binding protein rho regulates the assembly of focal adhesions and actin stress fibers in response to growth factors. *Cell* **70**, 389–399 (1992).
- Malliri, A. *et al.* The transcription factor AP-1 is required for EGF-induced activation of rho-like GTPases, cytoskeletal rearrangements, motility, and *in vitro* invasion of A431 cells. *J. Cell Biol.* **143**, 1087–1099 (1998).
- Manos, E. J. *et al.* Dolichol-phosphate-mannose-3 (DPM3)/prost-in-1 is a novel phospholipase C-gamma regulated gene negatively associated with prostate tumor invasion. *Oncogene* **20**, 2781–2790 (2001).
- Amit, I. *et al.* A module of negative feedback regulators defines growth factor signaling. *Nature Genet.* **39**, 503–512 (2007).
- Guo, W. & Giancotti, F. G. Integrin signalling during tumour progression. *Nature Rev. Mol. Cell Biol.* **5**, 816–826 (2004).
- Irie, H. Y. *et al.* Distinct roles of Akt1 and Akt2 in regulating cell migration and epithelial-mesenchymal transition. *J. Cell Biol.* **171**, 1023–1034 (2005).
- Geiger, B., Bershadsky, A., Pankov, R. & Yamada, K. M. Transmembrane crosstalk between the extracellular matrix–cytoskeleton crosstalk. *Nature Rev. Mol. Cell Biol.* **2**, 793–805 (2001).
- Rodrigue, C. M. *et al.* The cancer chemopreventive agent resveratrol induces tensin, a cell-matrix adhesion protein with signaling and antitumor activities. *Oncogene* **24**, 3274–3284 (2005).
- Kook, S. *et al.* Caspase-dependent cleavage of tensin induces disruption of actin cytoskeleton during apoptosis. *Biochem. Biophys. Res. Commun.* **303**, 37–45 (2003).
- Garcia-Alvarez, B. *et al.* Structural determinants of Integrin recognition by Talin. *Mol. Cell* **11**, 49–58 (2003).
- Wu, M. & Merajver, S. D. Molecular biology of inflammatory breast cancer: applications to diagnosis, prognosis, and therapy. *Breast Dis.* **22**, 25–34 (2005).
- Allred, D. C. *et al.* HER-2/neu in node-negative breast cancer: prognostic significance of overexpression influenced by the presence of *in situ* carcinoma. *J. Clin. Oncol.* **10**, 599–605 (1992).
- Xia, W. *et al.* Anti-tumor activity of GW572016: a dual tyrosine kinase inhibitor blocks EGF activation of EGFR/erbB2 and downstream Erk1/2 and AKT pathways. *Oncogene* **21**, 6255–6263 (2002).
- Spector, N. L. *et al.* Study of the biologic effects of lapatinib, a reversible inhibitor of ErbB1 and ErbB2 tyrosine kinases, on tumor growth and survival pathways in patients with advanced malignancies. *J. Clin. Oncol.* **23**, 2502–2512 (2005).
- Thiery, J. P. Epithelial–mesenchymal transitions in tumour progression. *Nature Rev. Cancer* **2**, 442–454 (2002).
- Zamir, E. *et al.* Dynamics and segregation of cell–matrix adhesions in cultured fibroblasts. *Nature Cell Biol.* **2**, 191–196 (2000).
- Albigez-Rizo, C., Frachet, P. & Block, M. R. Downregulation of talin alters cell adhesion and the processing of the  $\alpha 5 \beta 1$  integrin. *J. Cell Sci.* **108**, 3317–3329 (1995).
- Hazan, R. B., Qiao, R., Keren, R., Badano, I. & Suyama, K. Cadherin switch in tumor progression. *Ann. NY Acad. Sci.* **1014**, 155–163 (2004).
- Friedl, P. & Wolf, K. Tumour-cell invasion and migration: diversity and escape mechanisms. *Nature Rev. Cancer* **3**, 362–374 (2003).
- Sasaki, H., Yukiue, H., Kobayashi, Y., Fukai, I. & Fujii, Y. Cten mRNA expression is correlated with tumor progression in thymoma. *Tumour Biol.* **24**, 271–274 (2003).
- Sasaki, H. *et al.* Cten mRNA expression was correlated with tumor progression in lung cancers. *Lung Cancer* **40**, 151–155 (2003).
- Cui, Y., Liao, Y. C. & Lo, S. H. Epidermal growth factor modulates tyrosine phosphorylation of a novel tensin family member, tensin3. *Mol. Cancer Res.* **2**, 225–232 (2004).
- Calderwood, D. A. *et al.* Integrin $\beta$  cytoplasmic domain interactions with phosphotyrosine-binding domains: a structural prototype for diversity in integrin signaling. *Proc. Natl Acad. Sci. USA* **100**, 2272–2277 (2003).

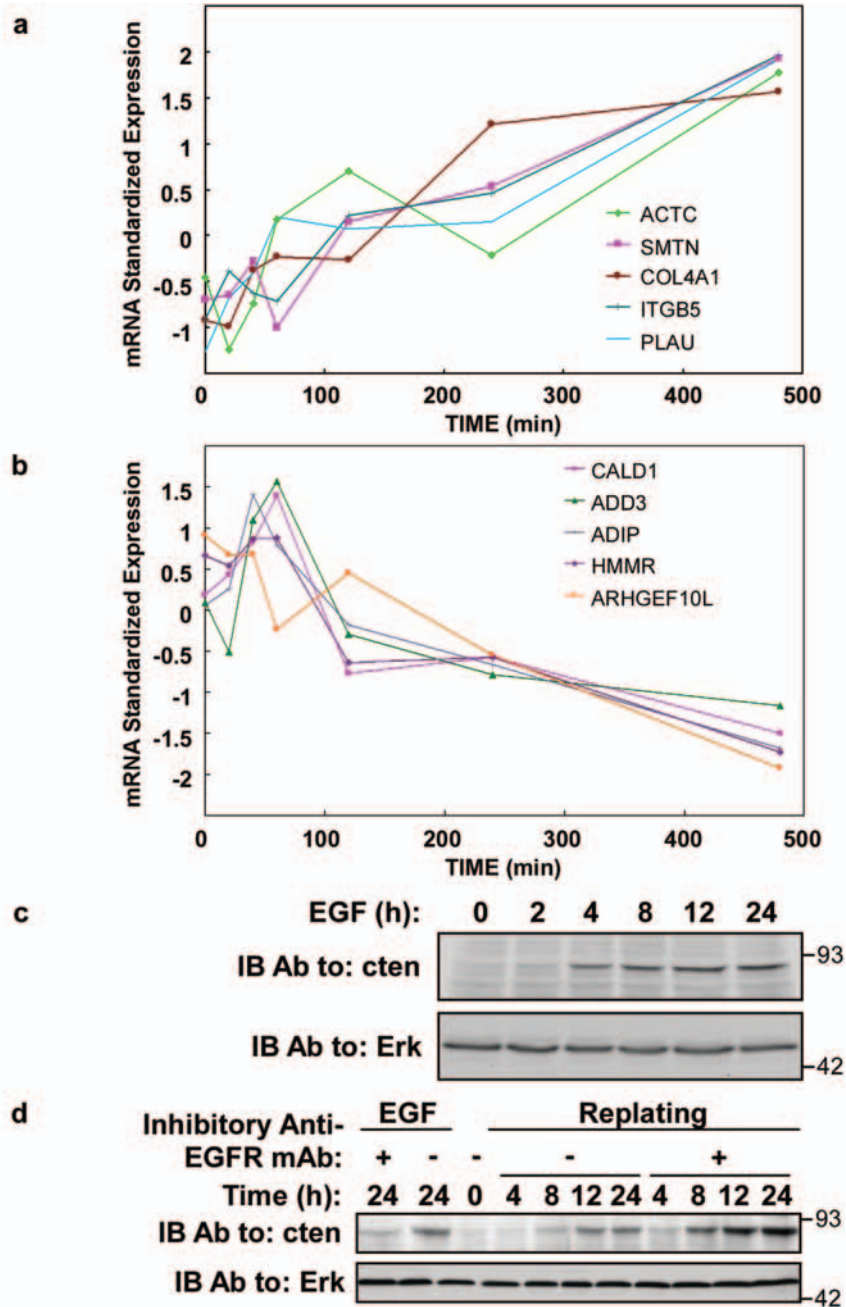


**Figure S1. EGF regulates transcription of migration-related genes, including cten.** (a, b) HeLa cells were stimulated with EGF (20 ng/ml) for the indicated time intervals and RNA analyzed using oligonucleotide arrays. Array values were standardized by subtracting the mean expression of each gene from its MAS5 expression values at the indicated time points, and the result divided by the standard deviation. Shown are standardized expression patterns of a selected group of motility related genes (presented as gene symbols). Both up- (a) and down- (b) regulated genes are presented. (c) HeLa cells were serum starved for 24 hours, and then incubated without or with EGF (20 ng/ml) for the indicated time intervals. Cells were then lysed and subjected to immunoblot analysis using a mouse anti-cten monoclonal antibody, or an anti-Erk2 antibody, as a protein loading control. (d) Serum-starved HeLa cells were trypsinized and re-plated in minimal medium, without or with an inhibitory anti-EGFR monoclonal antibody (40 µg/ml), for the indicated time intervals. For control, cells were incubated for 24 hours without or with EGF (20ng/ml), in the presence or absence of the inhibitory antibody. Whole cell extracts were subjected to immunoblotting (IB) with the indicated rabbit antibodies.

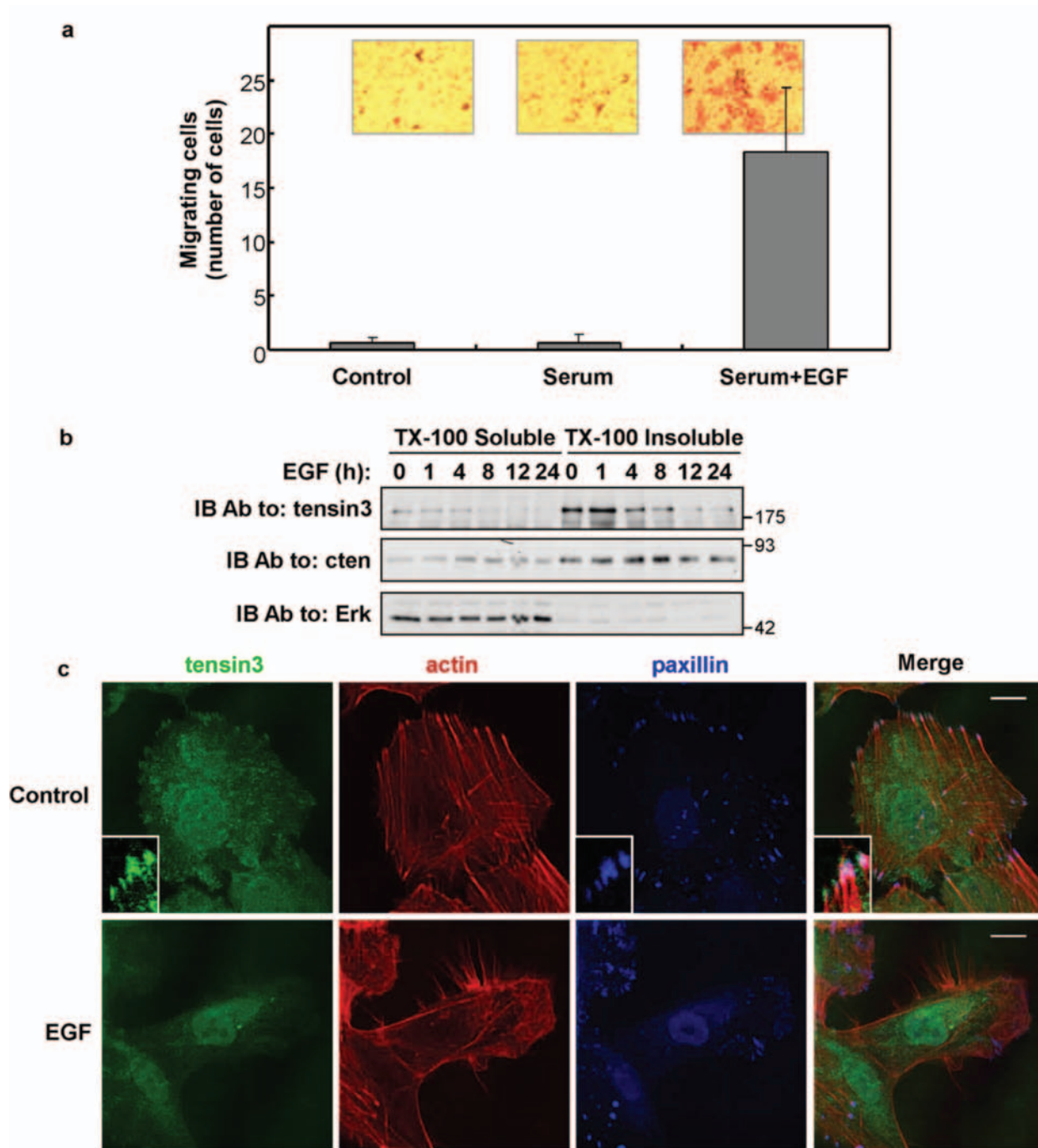


**Figure S2. EGF-induced MCF10A cell migration and stress fiber disassembly.** (a) MCF10A cell migration was analyzed by using the Transwell assay following incubation with minimal medium (*control*), serum-containing full medium without EGF, or EGF- and serum-containing full medium. Representative photomicrographs and quantification of migrating cells are presented. The indicated values are the average numbers (and S.D.; bars) of migrating cells per microscope field (n=6). (b) Serum-starved MCF10A cells were stimulated with EGF (10 ng/ml) for the indicated time intervals. Thereafter, cells were lysed using Triton X-100-based solubilization buffer and the supernatant was collected (*TX-100 Soluble*). Triton X-100 insoluble cell pellets were dissolved by boiling for 5 minutes in a buffer containing 1% SDS (*TX-100 Insoluble*). Cell lysates were further subjected to immunoblot analysis with the indicated antibodies. (c) Serum-starved MCF10A cells, were incubated without (*Control*) or with EGF for 24 hours. Thereafter, immunofluorescent analysis was performed using a rabbit anti-tensin3 antibody (green), TRITC-conjugated phalloidin (red) and a mouse anti-paxillin monoclonal antibody (blue). An overlay of the three fluorescence signals, generating white color in areas of co-localization, is shown in the right column. Enlargement of plasma membrane regions of cells stained for tensin3 and paxillin are presented (inserts). Bar, 10  $\mu$ m.

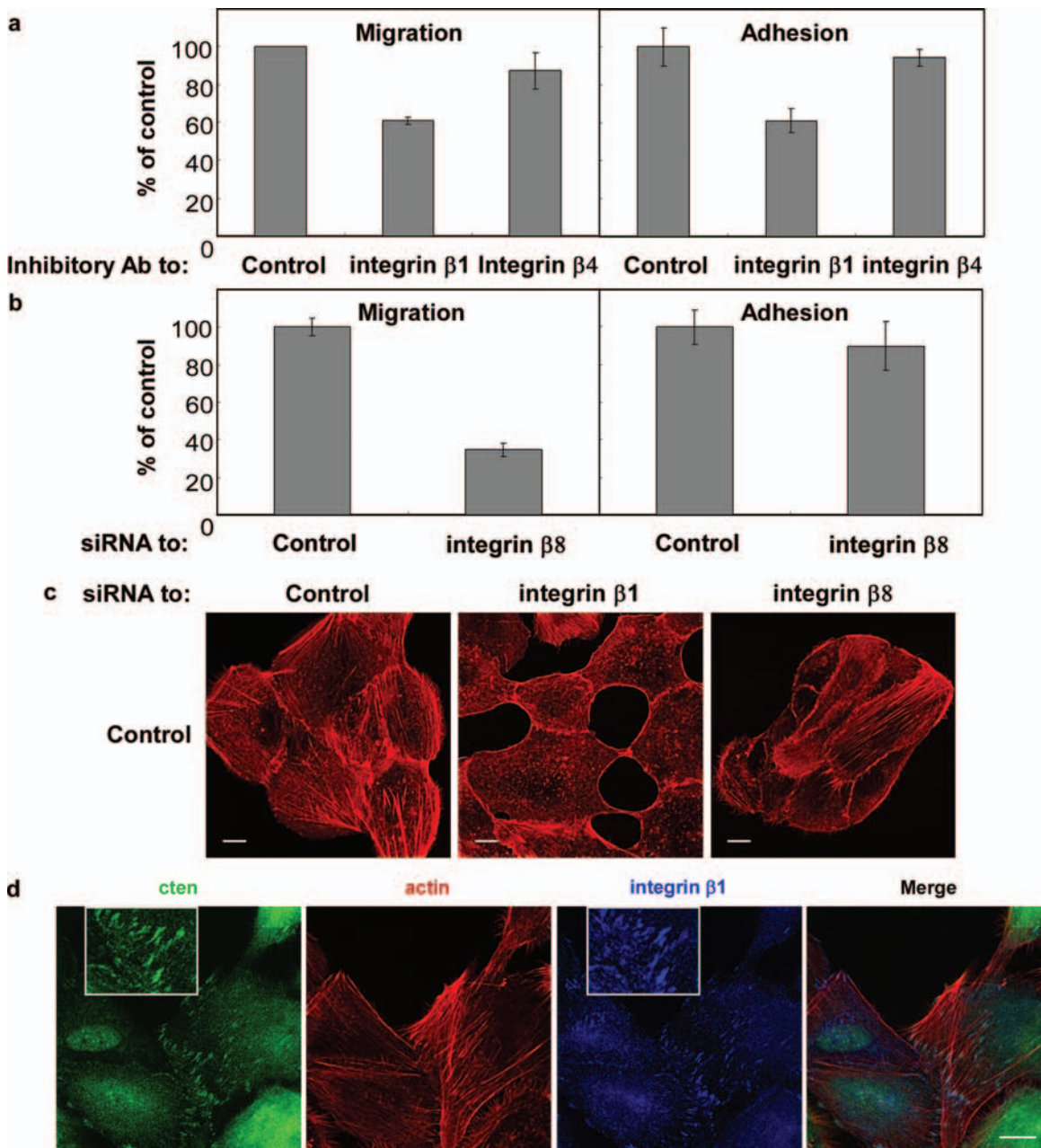


**Figure S3. Integrin beta-1 is essential for EGF-induced mammary cell motility.** (a) Migration panel: MCF10A cells were plated in a Transwell chamber in full medium supplemented with the following antibodies (each at 10  $\mu$ g/ml): Inhibitory anti-integrin beta-1 (P5D2; R&D Systems), inhibitory anti-integrin beta-4 (ASC-3; Chemicon), and normal mouse immunoglobulin G for control. Migration was measured and normalized to cells treated with a control antibody (n=2, bars represent S.D.). Adhesion panel: MCF10A cells were plated in a 96-well plate in full medium supplemented with the above indicated antibodies (10  $\mu$ g/ml). Two hours later, cells were washed. Adherent cells were stained with crystal violet and lysed in 10% SDS. Purple color representing the amount of adherent cells was determined using a spectrophotometer, and signals normalized to cells treated with a control antibody (n=5; bars,  $\pm$  S.D.). (b) Migration (left panel; n=4, bars represents S.D.) and adhesion assays (right panel; n=5, bars represent S.D.) were performed as in panel a using MCF10A cells transfected with either control siRNA oligonucleotides or integrin beta-8 oligonucleotides. (c) MCF10A cells transfected with the indicated siRNA oligonucleotides were grown in serum-containing medium (without EGF), prior to fixation and staining with TRITC-phalloidin. Bar, 10  $\mu$ m. (d) Serum-starved MCF10A cells were incubated without EGF for 24 hours. Thereafter, immunofluorescent analysis was performed using a rabbit anti-cten antibody (green), TRITC-conjugated phalloidin (red) or a mouse anti-integrin beta-1 monoclonal antibody (blue). An overlay of the three fluorescence signals, generating white color in areas of co-localization, is shown in the right column. Enlargement of plasma membrane regions of cells stained for cten and integrin beta-1 are presented in the inner boxes. Bar, 10  $\mu$ m.

SUPPLEMENTARY INFORMATION

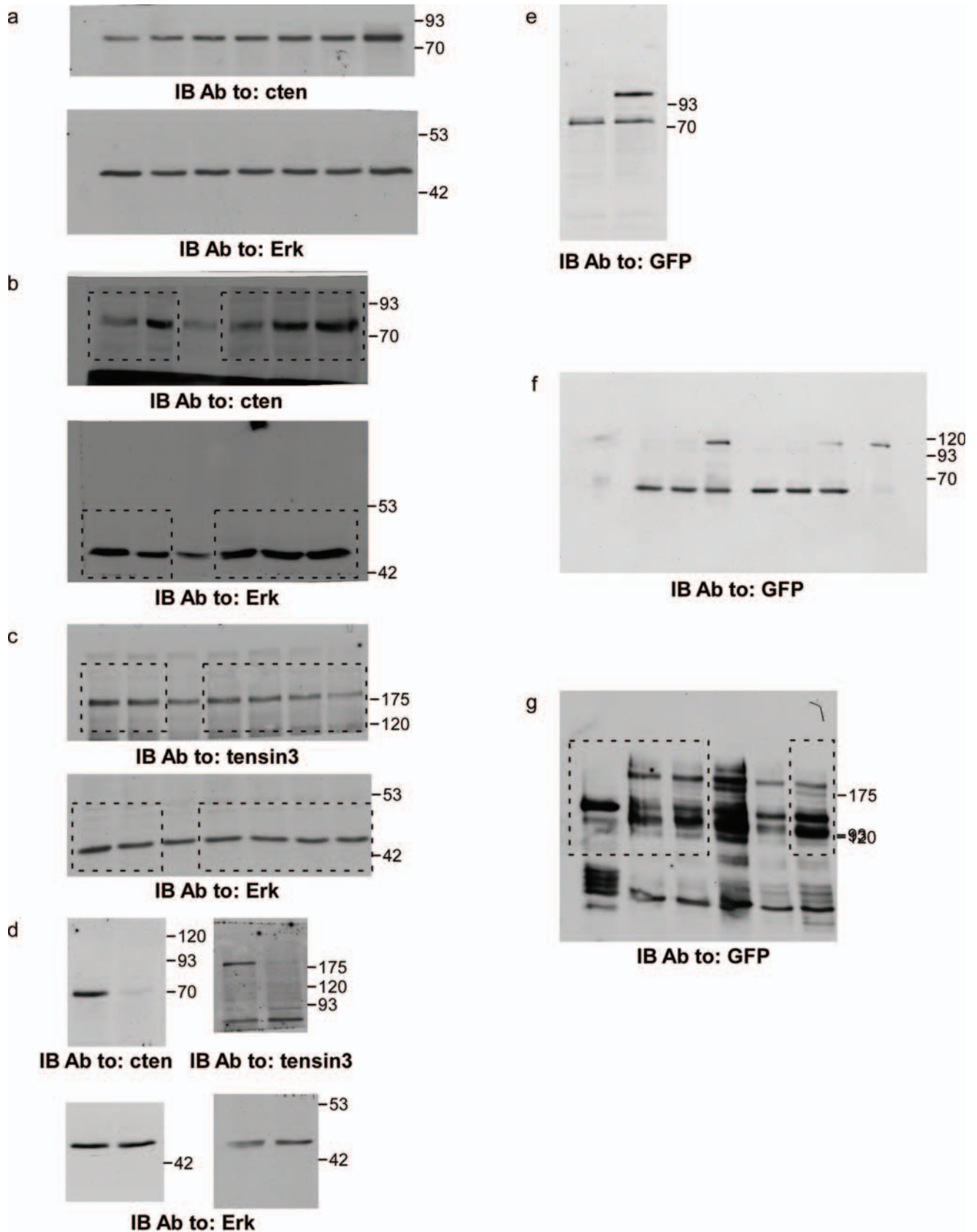


**Figure S4. Full scans of key immunoblot (western) data.** Shown are full scans of western data corresponding to the following figures: figure 1b (a), figure 1c (b; dotted boxes), figure 1d (c; dotted boxes), figure 2a (d), figure 3c (e), figure 4b (f), and figure 4d (g; dotted boxes).

**Supplementary Information Table S1. Association in IBC patients between the expression of cten and HER2, EGFR or pEGFR**

	Number of patients (total=18)	cten positive (N=10)	
		Association with cten positivity (%)	p-value
HER2 positive	18	56	
EGFR positive	14	71	0.023
Phospho-EGFR positive	11	91	<0.0001

Chi-Square test and the Fishers Exact test were used to assess the relationships between cten expression and either EGFR or phospho-EGFR.